

Development of Wave and Viscous Flow Analysis System for Computational Evaluation of Hull Forms

Wu-Joan Kim¹, Do-Hyun Kim¹ and Suak-Ho Van¹

¹ Marine Transportation System Research Center, Korea Research Institute of Ships and Ocean Engineering, Taejon, Korea; E-mail: shvan@kriso.re.kr

Abstract

A computational system for wave and viscous flow analysis(WAVIS) has been developed. The system includes a pre-processor, flow solvers and a post-processor. The pre-processor is composed of hull form presentation, surface mesh and field grid generation. The flow solvers are for potential and viscous flow calculation. The post-processor has graphic utility for result analysis. All the programs are integrated in a GUI-launcher package. To validate the developed CFD programs of WAVIS, the calculated results for modern commercial hull forms are compared with measurements. It is found that the results from WAVIS are in good agreement with the experimental data, illustrating the accuracy of the numerical methods employed for WAVIS.

Keywords: hull form, CFD, potential flow, viscous flow, wave, wake

1 Introduction

Computational Fluid Dynamics(CFD) technology has spread throughout the entire field of fluid engineering. Ship-building industry is not an exception. Recently some ship yards are trying to utilize computational tools for performance prediction in the basic design stage. But it is not easy to apply such commercial CFD packages to a modern practical hull form in spite of their versatility, since those are developed for general flow calculation. The successful application of CFD tool into the design of hull form depends upon usability as well as accuracy. The needs for a reliable numerical tool, which is concentrating upon the computation of flow around a ship hull and serving for initial hull form design, are emerging.

To cope with the aforementioned request, a computational system(WAVIS: WAVE and VIScous flow analysis system for hull form development) for flow calculation around modern commercial and naval ships has been developed with a user-friendly pre-processor, a robust turbulent flow solver as well as potential panel code, and a graphic post-processor. The most time consuming task to use a flow solver is known to be preparing surface and field meshes based on a given hull geometry. Programs for the presentation of hull surface using station offsets and for the generation of surface mesh have been developed. The field grid can be also obtained by solving the Poisson equation with surface meshes and prescribed boundary topologies. A potential panel method using Rankine source has been developed to solve wave-resistance problem with the linear and nonlinear free surface condition. A robust Reynolds-averaged Navier-Stokes solver is employed to provide

all the turbulent flow information such as surface pressure and velocity field at the propeller plane, etc. All of the above programs and a post-processor having graphic utilities are integrated in a GUI-launcher program operating in a PC. To validate the developed computational tool, it is essential to confirm the calculated results against the reliable experimental data. KRISO recently provided well-documented flow information around modern commercial ships, namely 3600TEU Container Ship(KCS) and 300K VLCCs(KVLCC, KVLCC2), both of which were selected for the test cases in Gothenburg 2000 CFD Workshop. The obtained computational results from WAVIS for KCS and KVLCCs are compared with the experiment to confirm the reliability and accuracy of developed numerical methods.

2 Computational system(WAVIS)

2.1 GUI-Launcher

WAVIS has the functions of hull form definition, surface mesh generation, field grid generation, potential flow calculation and viscous flow calculation, as depicted in Figure 1. For the integration of the developed CFD programs, a Windows-based launcher program is utilized. The main objective of the launcher is to provide user-friendly environment for computation and analysis. Nine Fortran console program modules are integrated, namely, Offset View, X-station, Surface Mesh, FS Panel Gen, Potential Solver, Field Grid O-O, Field Grid O-H, Viscous Solver and Wake Analysis. Input dialog window is provided to enter the parameters conveniently on each program module. As the input parameters are ready, the launcher program send a command to execute the Fortran console programs. The results from each program can be analyzed immediately by using graphics utility designed for flow analysis. It is sometimes preferred to execute flow solvers in remote workstations. Launcher provides a socket program communicating with remote machines to transfer data files and to receive results. In Figure 2 a typical input window in GUI-launcher is shown.

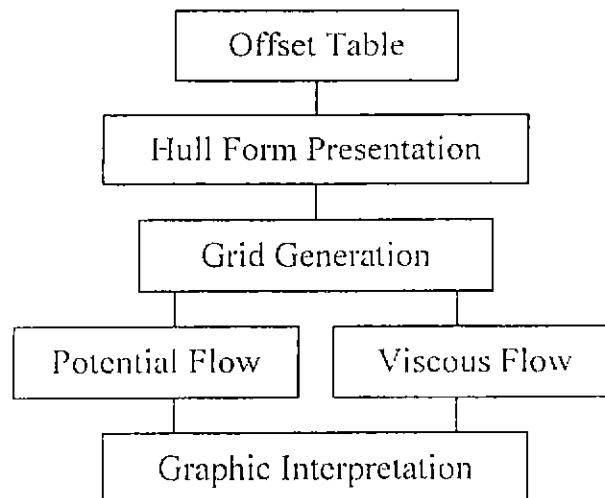


Figure 1: Modules of WAVIS

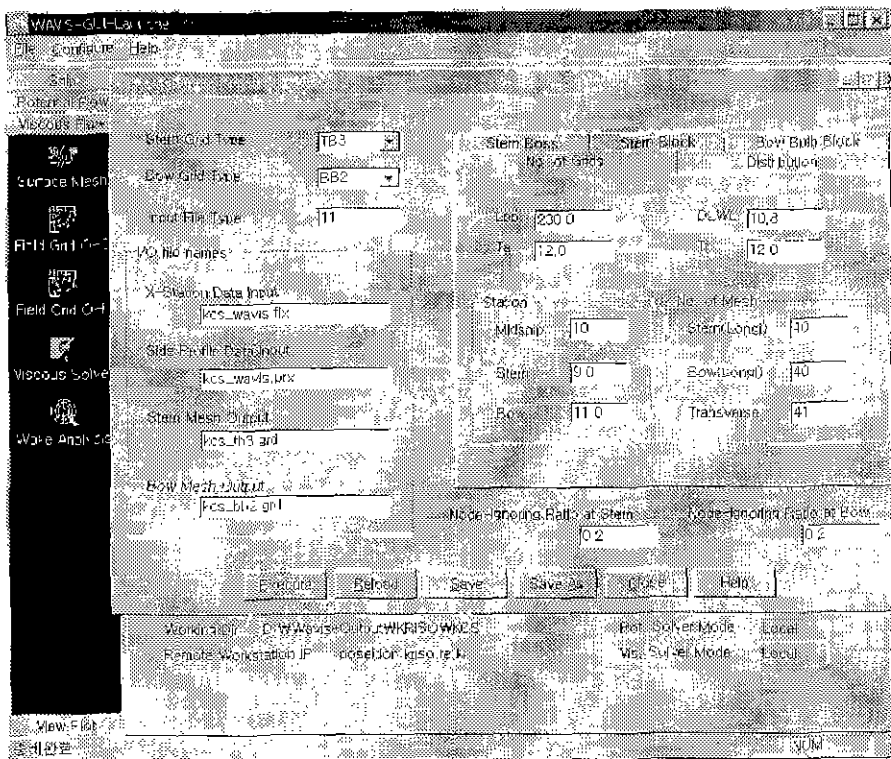


Figure 2: WAVIS-Launcher input window

2.2 Pre-processor

2.2.1 Hull form definition and surface mesh generation

It is cumbersome to describe a modern hull form by using only the offset table, since the complexity of bow and stern shapes always requires more information. To make it easy and quick to present hull form and generate surface meshes with acceptable accuracy, the user-friendliness is emphasized in the newly developed program. In the present study focus is laid on commercial ships such as tanker, bulk carrier and container ship with bulbous bow and stern bulb, as well as naval ships. The procedures for hull form definition and surface mesh generation are described in the followings.

The most important input data is an offset table provided by the designer. The offset table usually contains the offset points of 25~30 stations and the centerline profiles of bow and stern. The developed program converts automatically the offset table into the proper form containing slope-controlling integers at every special points of discontinuous slope or curvature. After the file conversion is completed, non-uniform parametric spline with Ferguson basis is utilized to generate sufficiently many interpolated points for the body plan and the side profile. This procedure is implemented in the Offset View module of WAVIS.

As it is well known, more information than in the offset table is required to construct complicated bow and stern shapes. Thus, it is necessary to determine additional station offsets near the bow and the stern. In the X-station module of WAVIS, waterlines are defined to specify additional

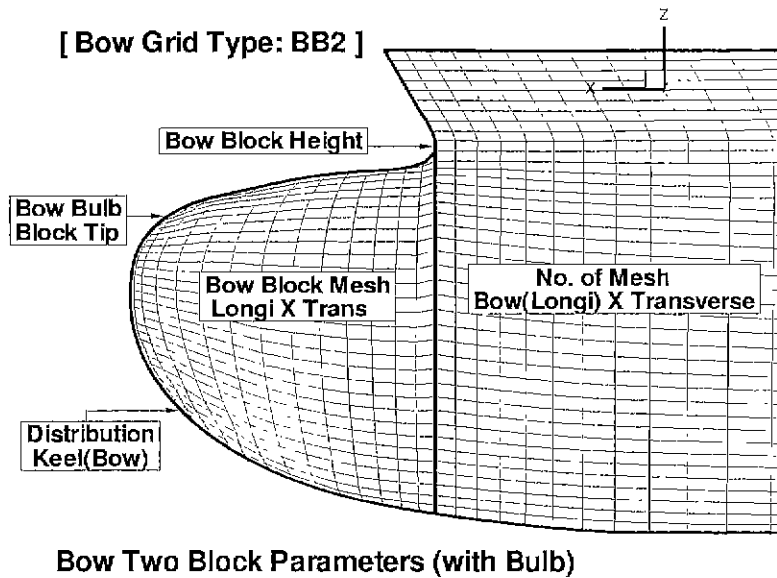
station offsets. But the shapes of waterline ending are usually not clarified in the original station offset. However, it is possible to define the end shapes of waterline near the bow and the stern by using the predetermined parameters, which choose waterline endings from natural spline, normal spline, ellipse, parabola, hyperbola, and their combination. After the waterlines are obtained, additional stations near the stern and the bow can be generated using the waterline intersection points at the constant longitudinal location. Detailed information on the stations near bow and stern is sometimes available from other CAD programs such as HCAD, etc. WAVIS can accept such CAD data to define hull form instead of making detailed offset points.

Surface meshes are generated by connecting detailed offset points appropriately in the Surface Mesh module of WAVIS. Three bow types are defined, i.e., single block topology with and without bow bulb, and two block topology with bow bulb. On the other hand, surface mesh for stern region is rather complicated, depending on cruise and transom stern, with and without stern bulb, single, two and three block topology. Users can choose bow and stern mesh types, which invoke separate routines for different topology on various hull forms. To make the surface mesh flexible, the longitudinal and transverse distribution can be arbitrary adjusted with the girth length ratio. This efficient hull surface mesh generator will improve the usability of available computational tools for the hull form evaluation. Figure 3 shows the generated hull surface mesh for a container ship. For the details of the present procedures, see Kim et al(1998a) and Kim and Van(1999). Generated surface meshes can be used immediately as hull surface panels for potential flow calculation, or as boundary surface grids in three-dimensional field grid generation for viscous flow calculation.

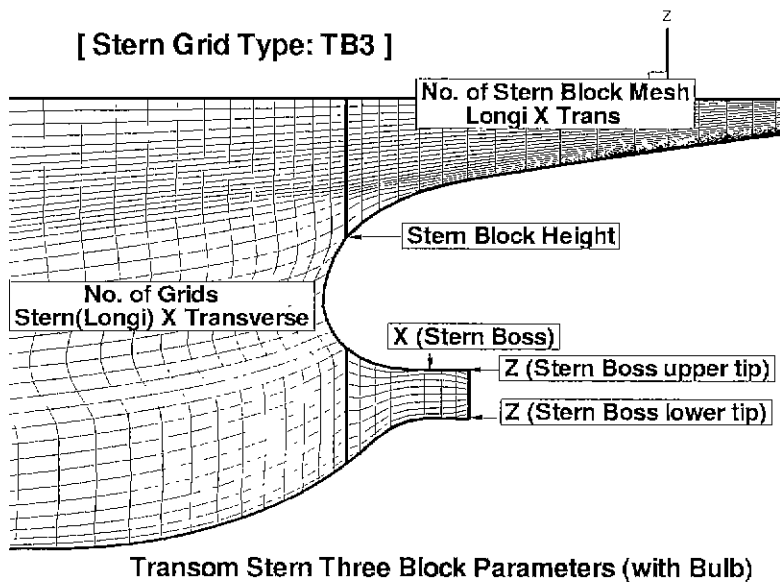
2.2.2 Field grid generation

In WAVIS two field grid topologies of O-O and O-H are implemented in Field Grid O-O and Field Grid O-H modules, respectively. It is more economical to use O-O topology to calculate turbulent flow around a ship hull, since less grids are distributed along the symmetry boundaries. However, O-O type grid system often deteriorates the robustness of viscous solver. On the other hand, O-H topology is more convenient in treating transom stern. To provide more reliable viscous flow solving system, both O-O and O-H type grid topologies are adopted in WAVIS. Information on surface mesh is automatically transferred to Field Grid Generating module, in which 3-D Poisson equations are solved to constitute field grid system with predetermined grid interval and intersecting angle at hull surface boundary.

Among boundary surfaces in 3-D field grid system, the hull surface mesh is already given. The two-dimensional grid systems on other planes of symmetry are obtained by solving 2-D Poisson equations. After constituting all boundary surfaces, it is possible to use the algebraic method like trans-finite interpolation(TFI) to fill out the inside grid system. It is rather simple, but does not guarantee the normality of grid on the hull surface. In WAVIS the 3-D Poisson equations are solved to meet the requirement of grid orthogonality and controllability. Sorenson's method(1980) is extended into three-dimension to define the grid-control function of Poisson equations. Since the initial guess for the Poisson iterative solver for grid generation is usually very poor, much attention should be paid to the robustness of Poisson solver. In WAVIS the Poisson equation is discretized by using the weighting function scheme and resulting linear equations are solved by the modified strongly implicit procedure, details of which are given in Kim et al(1999a). An example of field grid system for a VLCC is shown in Figure 4.



(a) Bow grid type: BB2



(b) Stern grid type: TB3

Figure 3: Generated surface mesh near bow and stern region of a container ship by WAVIS

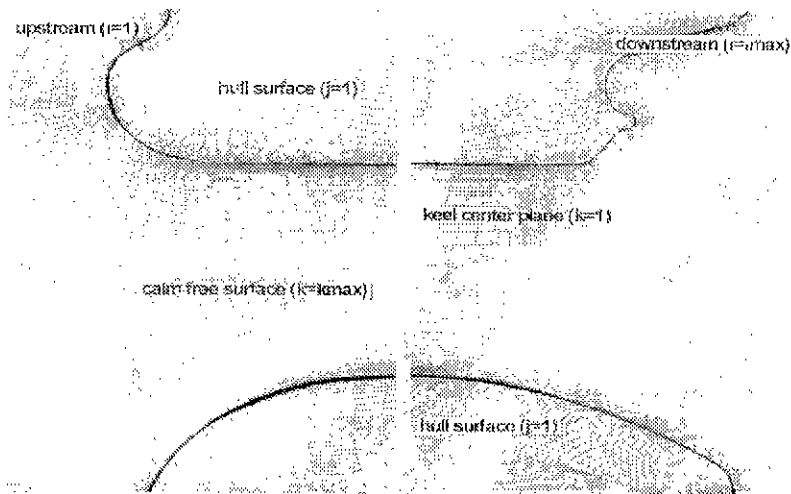


Figure 4: Generated field grid system around a VLCC by WAVIS

2.3 Flow solvers

2.3.1 Potential flow solver

The wave resistance and wave pattern can be predicted using the Potential Solver module of WAVIS. It is possible to perform viscous flow calculation with free surface, however, it is too expensive to use in daily basis. Thus, in WAVIS, the wave resistance problem is treated by the following potential flow solver.

The Rankine source method is adopted to perform the potential flow calculation of practical hull forms and the raised panel approach (Raven 1992) is used for handling the nonlinear free surface condition. To enforce the radiation condition the present Rankine source method employs 4-point upwind-difference operator. Furthermore, upstream collocation points are shifted to smooth out the source strengths and to prevent upstream waves at high speeds. To speed up the convergence in iterative procedures for nonlinear free surface flow calculation, the preconditioned GMRES technique is employed. Pressure integration method is utilized to calculate the wave resistance. For the application to practical hull forms with the large bow flare, flat stern overhang and transom stern at low speeds, much attention is paid to provide reasonable solution. The dry transom model is employed to treat transom stern. Trim and sinkage can be also predicted in full load and ballast conditions. The details of the present panel method can be found in Kim et al (1998b).

2.3.2 Viscous flow solver

The viscous resistance such as frictional drag and form drag can be calculated by using the Viscous Solver module of WAVIS. Nominal wake distribution at the propeller plane can be also predicted, which is very useful to judge the propulsive performance of a ship.

For the computation of turbulent flow, the Reynolds-Averaged Navier-Stokes (RANS) equations are solved by the semi-implicit finite-volume method. For the turbulence closure, the real-

izable k-epsilon model is exploited. The wall proximity effect is avoided by employing the wall function bridging the wall region and the fully turbulent region. The numerical method employs the QUICK scheme for convection terms, and the central-difference scheme for diffusion terms. To obtain the pressure field, the SIMPLEC method are utilized to ensure the divergence-free velocity field. The non-staggered grid system is chosen for simplicity and an artificial dissipation for pressure equation is added to suppress the pressure oscillations. Linear equations are solved by using strongly implicit procedures. To avoid unstable behavior during the initial stage of iteration when flow starts abruptly, initial pressure and velocity components are given from double body potential flow solution. It is also possible to start from the previously obtained similar solutions. For details, see Kim et al(1999b).

2.4 Post-processor

After the solution of potential and viscous flow calculation is achieved, it is necessary to investigate the results. The WAVIS includes flow analyzing tools connected to Tecplot graphics package. For potential flow, the wave elevation along the hull surface and wave patterns are given. Wave profiles along a longitudinal cut are also available. Surface pressure and velocity vectors on hull surface from potential solution can be displayed.

For the viscous flow solution, frictional and form drag are calculated. Velocity distribution at the propeller plane can be examined by simply entering a few parameters about propeller position. Wake analysis tools will provide axial velocity contours and transverse vectors. Radial and transverse distribution of wake can be also given as well as harmonic analysis results. Limiting streamlines and pressure distribution on the hull surface can be displayed easily. The flow information obtained in post-processing is valuable for the improvement of hull form. Furthermore, a series of hull form variation along with the comparison of computational results will guide the designer to determine the final hull form effectively at low costs.

3 Validation with experiments

To validate the developed computational tools, two well-documented data base are utilized, namely KRISO 3600 TEU Container Ship(KCS)(Van et al. 1998a) and two 300K VLCC's (KVLCC, KVLCC2) (Van et al. 1998b), which are selected for the test case of Gothenburg 2000 CFD Workshop. It is meaningful to make comparison on these hull forms, since those are very similar to modern commercial hull forms. The Reynolds numbers in the test are 1.4×10^7 and 4.6×10^6 , while the Froude numbers are 0.260 and 0.142 for the container ship and the VLCC, respectively. The calculated wave patterns and local mean velocity components and nominal wake distribution are compared with the experiments. The Cartesian coordinates (X, Y, Z) are used for displaying the data, where X denotes the downstream direction, Y starboard, and Z the upward direction. The origin of the coordinates is located at the midship and calm free surface. All the quantities are non-dimensionalized by the speed and the length between perpendiculars(L_{pp}) of the model ship.

3.1 Wave patterns

The developed potential panel method is applied to calculate wave resistance and wave patterns for KCS and KVLCC are generated. The calculation is performed after modification of transom stern.

since the effect of transom does not appear clearly for the present case. First, the potential flow around KCS at $Fn=0.260$ with the nonlinear free surface condition is performed. 80×16 panels are distributed on the hull surface, while 118×16 panels are used on the free surface, corresponding to 20 panels per a fundamental wave length. The calculated wave pattern is compared with the measured data in Figure 5. The prediction is in close agreement with the experimental data. Figure 6 shows the comparisons along the longitudinal cuts at $Y/L_{pp}=0.1024, 0.1509, 0.2167$, respectively. A fairly good agreement is illustrated in these figures except peaks near crest and trough. In the next, the wave pattern around KVLCC at $Fn=0.142$ is calculated. 80×16 panels are used for the hull surface, but 213×16 free surface panels are distributed, since the Froude number is very low. As a result, 15 panels per a fundamental wave length are used. The calculated results are compared with the measured data in Figure 7 for $Y/L_{pp}=0.1169, 0.2086$. The bow wave systems are well predicted, although a little bit of discrepancies near parallel middle body are seen. It is believed that the agreement shown in the present paper is one of the best among the published potential flow solution for practical hull forms.

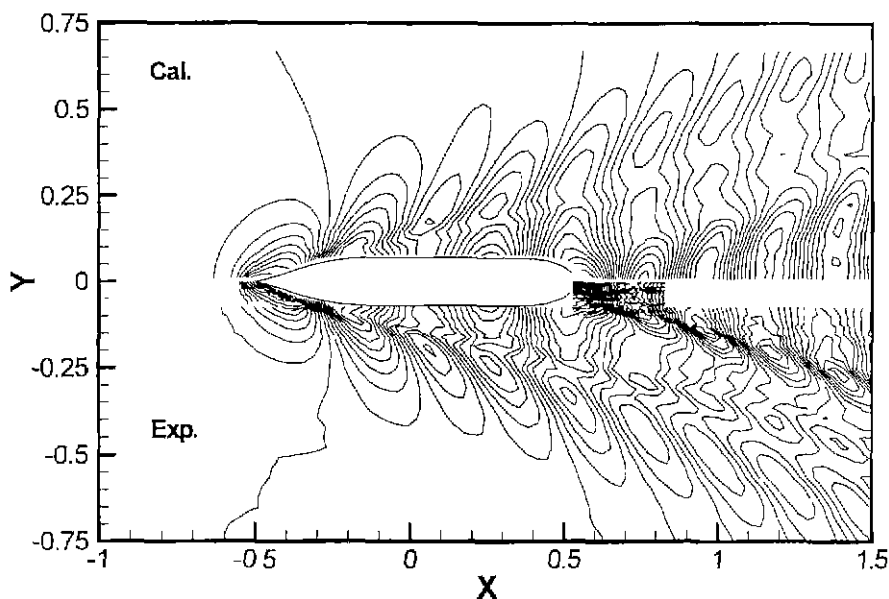
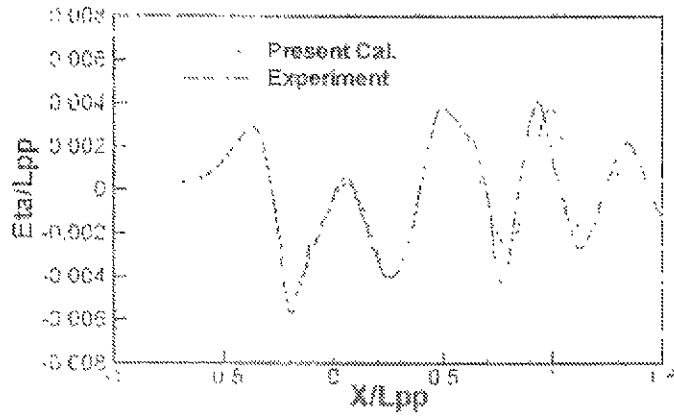


Figure 5: Comparison of wave pattern around KCS($Fn = 0.26$)

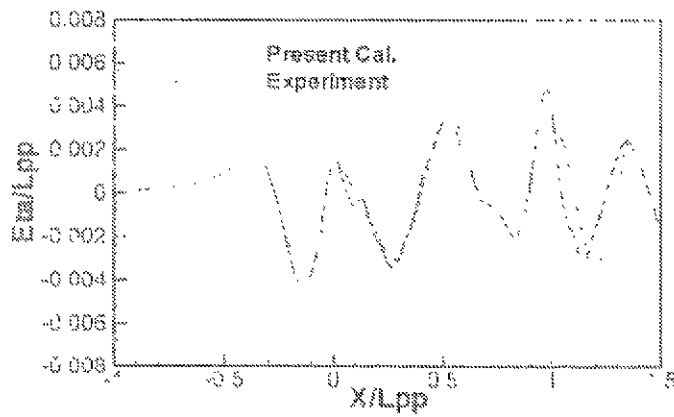
3.2 Wake distribution

The grid generator and turbulent flow solver described in the preceding sections are applied for two KVLCC hull forms. $97 \times 33 \times 33$ grids are used with the first grid interval of 0.5×10^{-4} . The axial velocity distributions at stern stations are compared with experiments. It should be noted that the measurements were carried out in towing tank, thus, flow field was probably affected by wave generation on the free surface. However, the present calculation ignores the effect of waves, since the Froude number of the present calculation is 0.142. Instead, Neumann condition is applied on the calm free surface.

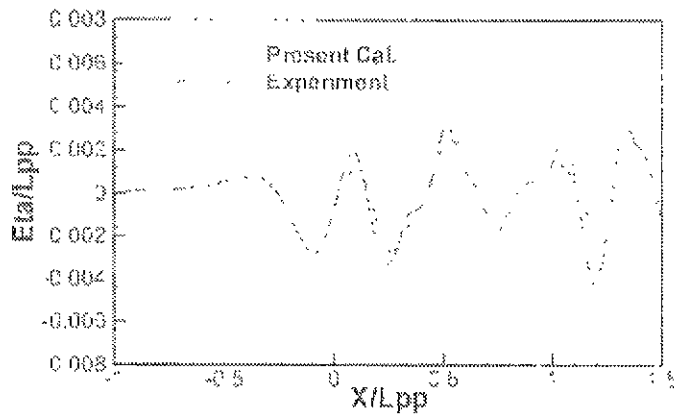
In Figures 8 and 9 the calculated velocity field at St. 2 and St. 0.35 of KVLCC is in good



(a) $Y/L_{pp} = 0.1024$



(b) $Y/L_{pp} = 0.1509$



(c) $Y/L_{pp} = 0.2167$

Figure 6: Wave profiles along longitudinal cuts for KCS ($Fn = 0.26$)

agreement with the experiment. Main features of thick boundary layer flow are well depicted, and the present computational model provides realistic wake distribution with hook-like shape. However, it is more important to find out whether the calculated results provide the right information on the changes in wake distribution due to stern frameline modification. For that purpose, the comparison is made for KVLCC and KVLCC2, which have the same forebody and slightly different afterbody. KVLCC2 has more U-shaped stern framelines which implies the formation of stronger bilge vortices, as can be noticed from Figure 10. The difference of wake distribution at the propeller plane of two hull forms are well predicted in WAVIS. It is very encouraging to see that calculated results predict the flow and the difference as well. The radial distribution of circumferentially averaged axial velocity components are compared in Figure 11, showing clearly the effect of stern hull form variation on nominal wake distribution. The present results provide new hope for CFD to be applied in ship resistance and propulsion problem.

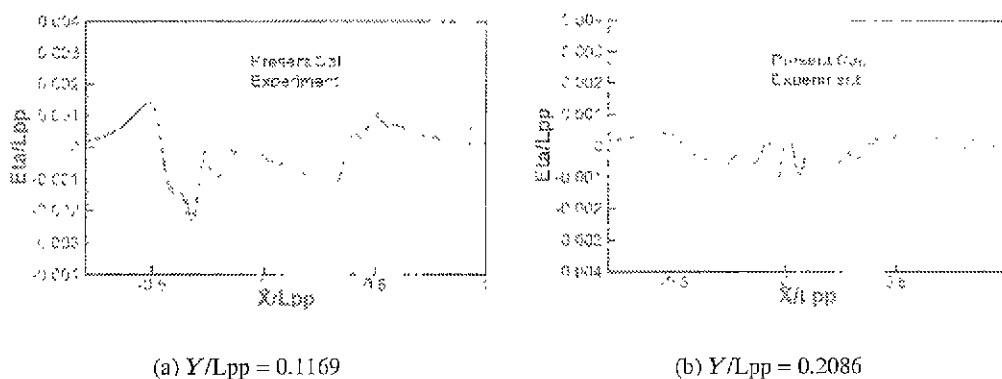


Figure 7: Wave profiles along longitudinal cuts for KVLCC ($Fn = 0.142$)

4 Concluding remarks

A computational system(WAVIS) for the hull form evaluation is developed to provide an efficient numerical tool in the basic hull form design. The system includes a pre-processor, flow solvers, and a post-processor. Fortran programs for hull form presentation, surface mesh and field grid generation, and potential and viscous flow calculation are integrated into one unit with GUI launcher. To validate the developed CFD programs, the calculated wave patterns and local velocity fields are compared with the towing tank experiment for practical hull forms. The calculated results are in good agreement with experiment, proving the accuracy of the numerical methods employed in WAVIS. It is believed that the developed program can be a useful computational tool for the hull form evaluation in the initial hull form design stage.

Acknowledgement

The present work is based on the projects of "Improvement of Resistance Performance of Ships," supported by Ministry of Industry and Resources, and "Development of Hydrodynamic Perfor-

KRISO 300K VLCC(F1+A1)

St. 2

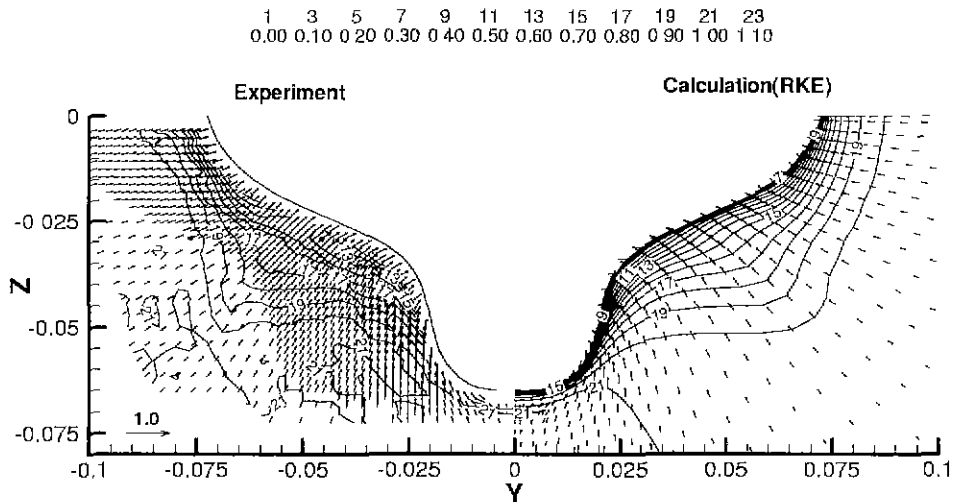


Figure 8: Comparison of velocity field at St. 2 of KVLCC($Re=4.6 \times 10^6$)

mance Analysis System.” supported by Ministry of Science and Technology.

References

- KIM, W.J. ET AL 1998a A computational study on turbulent flow around a practical hull form with efficient grid generator. Proc, Third Osaka Colloquium on advanced CFD application to ship flow and hull form design, Osaka, Japan
- KIM, D.H., KIM, W.J., VAN, S.H. AND KIM, H. 1998b Calculation of potential flow around modern commercial ships using nonlinear free surface condition. Proc, Third Int'l Conf on Hydrodynamics, Seoul, Seoul, Korea
- KIM, W.J., KIM, D.H. AND VAN, S.H. 1999a Development of 3-D field grid generating method for viscous flow calculation around a practical hull form. J. of Society of Naval Architects of Korea, **36**, 1, pp. 70-81
- KIM, W.J., KIM, D.H. AND VAN, S.H. 1999b Calculation of turbulent flows around VLCC hull forms with stern frameline modification. Proc, the 7th Numerical Ship Hydrodynamics, Nantes, France
- KIM, W.J. AND VAN, S.H. 1999 Practical method for generating surface mesh using offset table. J. of Society of Naval Architects of Korea, **36**, 1, pp. 61-69
- RAVEN, H.C. 1992 A practical nonlinear method for calculating ship wave making and wave resistance. Proc, the 19th Symp on Naval Hydrodynamics, Seoul, Korea

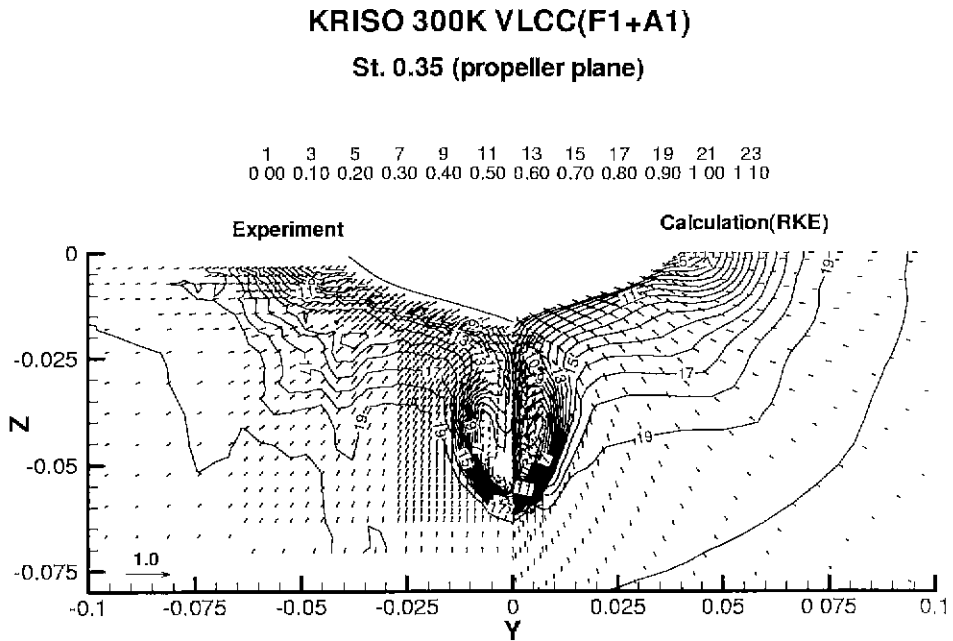


Figure 9: Comparison of velocity field at St. 0.35 of KVLCC($Re=4.6 \times 10^6$)

- SORENSEN, R.L. 1980 A computer program to generate two-dimensional grids about airfoils and other shapes by the use of Poisson equation. NASA TM 81198
- VAN, S.H. ET AL 1998a Experimental investigation of the flow characteristics around practical hull forms. Proc, Third Osaka Colloquium on advanced CFD applications to ship flow and hull form design
- VAN, S.H. ET AL 1998b Experimental study on the flow characteristics around VLCC with different stern shapes. Proc, Third Int'l Conf on Hydrodynamics, Seoul, Korea

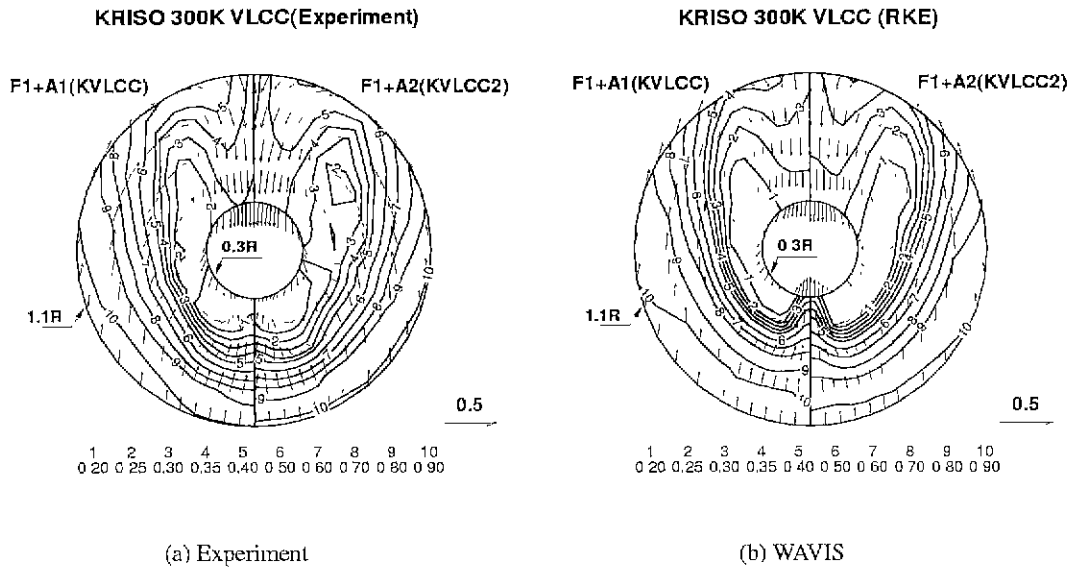


Figure 10: Wake distribution at propeller plane of KVLCC and KVLCC2

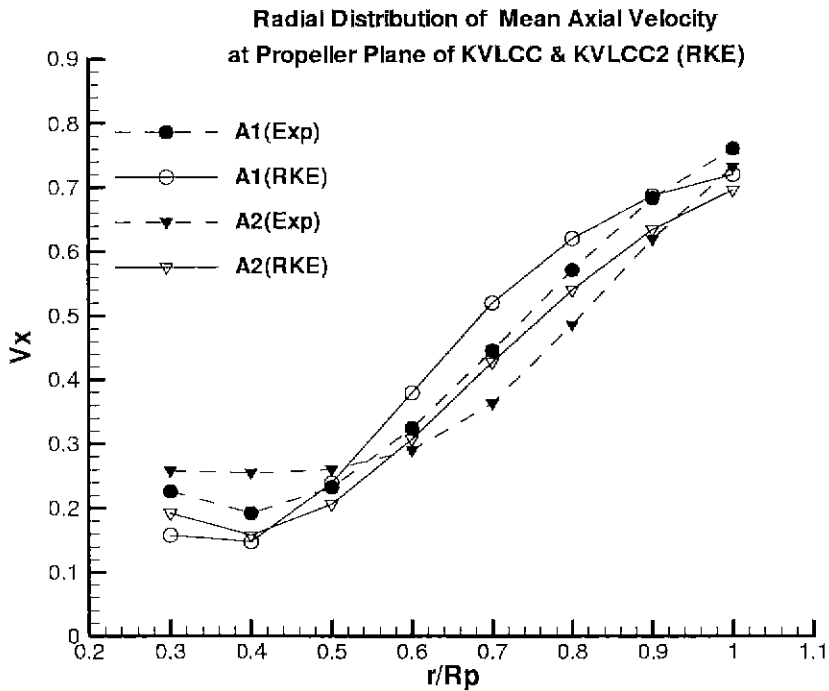


Figure 11: Comparison of axial velocity distribution of KVLCC and KVLCC2 at the propeller plane